

Ferrimagnets with Ising ions. H - T - x phase diagrams of holmium-yttrium iron garnets

G. A. Babushkin, A. K. Zvezdin, R. Z. Levitin, A. I. Popov, and V. I. Silant'ev

Moscow Institute of Electronic Technology

(Submitted 21 August 1980)

Zh. Eksp. Teor. Fiz. 80, 1952-1962 (May 1981)

The magnetization of single crystals of holmium-yttrium iron garnets $\text{Ho}_x\text{Y}_{3-x}\text{Fe}_5\text{O}_{12}$, for various concentrations x ($0.25 \leq x \leq 1.63$), has been measured in fields up to 300 kOe over the temperature range from helium to nitrogen temperatures. Experimental H - T - x diagrams have been plotted. On the basis of the Ising model for the Ho^{3+} ions [V. I. Silant'ev, A. I. Popov, R. Z. Levitin, and A. K. Zvezdin, Sov. Phys. JETP 51, 323 (1980)], magnetic phase transformations in this system are investigated theoretically as functions of H , T , and x for three orientations of the magnetic field: $\mathbf{H} \parallel \langle 111 \rangle$, $\mathbf{H} \parallel \langle 110 \rangle$, $\mathbf{H} \parallel \langle 001 \rangle$. The theoretical results are compared with experimental data. The reasons for differences between them in a number of cases are discussed.

PACS numbers: 75.30.Kz, 75.40.Dy, 75.50.Gg

Earlier,¹ investigations were made of field-induced orientational phase transitions in holmium-yttrium iron garnets (HYIG), of composition $\text{Ho}_x\text{Y}_{3-x}\text{Fe}_5\text{O}_{12}$, at 4.2 K. It was discovered that the transitions occur discontinuously and can be described with an Ising model of the behavior of the magnitude moments of the Ho^{3+} ions. It follows from this model that the magnetic moments of the Ho^{3+} ions, which form three rare-earth (RE) sublattices, can be oriented only collinearly with certain Ising axes, parallel to crystallographic axes of the $\langle 100 \rangle$ type, whatever the value of the external magnetic field \mathbf{H} . The anomalies observed on the magnetization curves are explained by reorientation of the moments of the RE ions through π radius during the corresponding change of orientation of the magnetization of the iron sublattice; the picture of the transitions depends in a substantial way on the concentration of RE ions Ho^{3+} .

In the present paper, magnetic H - T phase diagrams are investigated experimentally for various concentrations x of the ions, and a theoretical calculation of these diagrams is made with a model that allows for the Ising character of the Ho^{3+} ions. The theoretical results are compared with experimental data. An analysis is made of the possible reasons responsible for differences, in a number of cases, between the experimental and the theoretical data.

1. EXPERIMENTAL RESULTS

The principal methods of investigation were measurements of the magnetization M and of the susceptibility of HYIG crystals in pulsed fields up to 300 kOe. The transition fields were determined from the curves of susceptibility vs field. The specimens and the experimental methods have been described earlier.^{1,2} Our measurements show that with rise of the temperature T , the jumps on the magnetization curves are smeared out, decreasing in magnitude, and that on attainment of a certain critical temperature T_{cr} they disappear. The peaks on the susceptibility curves shift along the H axis and also disappear on attainment of T_{cr} . Diagrams of the temperature dependence of the transition fields at composition $x=0.67$, for magnetization along axes

$\langle 100 \rangle$, $\langle 110 \rangle$, and $\langle 111 \rangle$, are given below, in Fig. 1. The light circles on the figure correspond to increase of the field, the dark to decrease. The number of transitions, for magnetization along each of the three axes, does not change with temperature. Similar diagrams are observed for all compositions with $x < x_c = 0.8$, where x_c is the concentration at which the magnetization of the specimen at 0 K, in the absence of an external field, is zero.

The phase diagrams for $x > x_c$ have a different character. Below, Fig. 2 shows diagrams of the temperature dependence of the transition fields for composition $x=1.05$. In this case, jumps on the magnetization

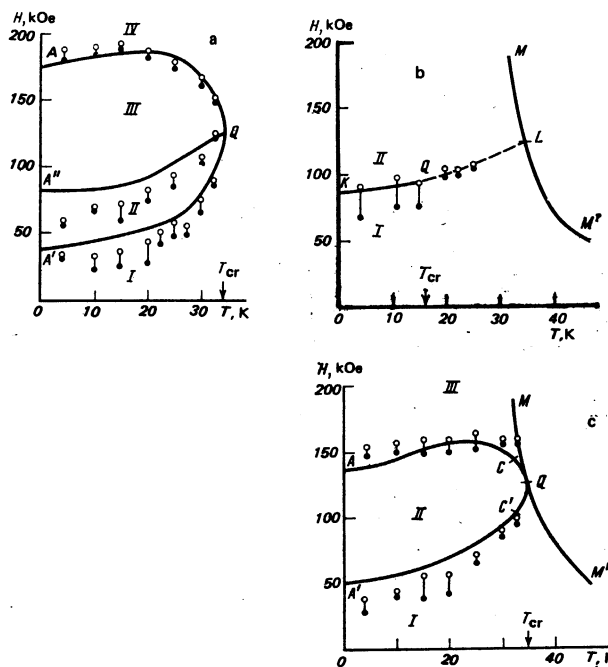


FIG. 1. H - T - x phase diagrams for HYIG when $x=0.67$: a, $\mathbf{H} \parallel \langle 111 \rangle$; b, $\mathbf{H} \parallel \langle 110 \rangle$. Solid lines: theory. Light circles were obtained with increase of the field during the measurement process, dark circles with decrease of the field. The dotted line in Fig. 1b is described by equation (3).

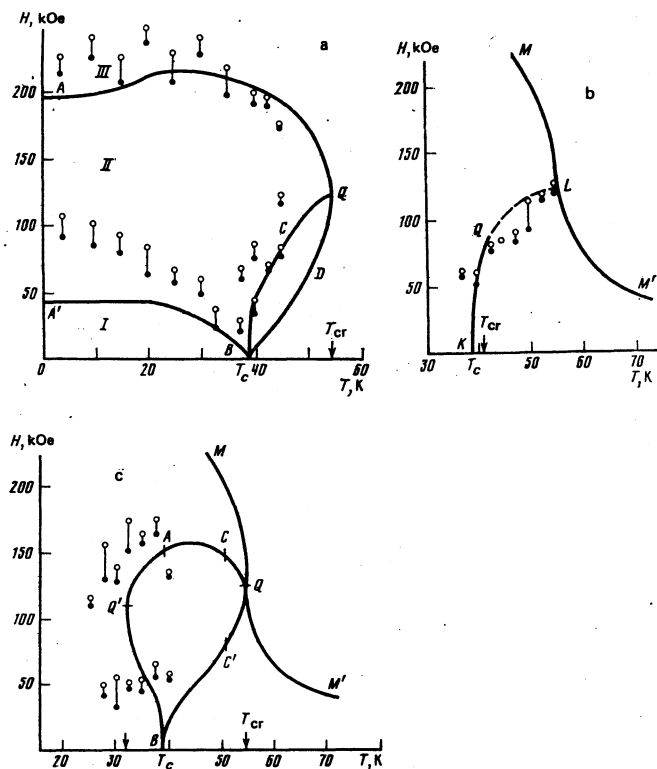


FIG. 2. H - T - x phase diagrams for HYIG when $x=1.05$: a, $H \parallel \langle 111 \rangle$; b, $H \parallel \langle 110 \rangle$. Solid lines: theory. Light circles were obtained with increase of the field during the measurement process, dark circles with decrease of the field. The dotted line in Fig. 2b is described by equation (3).

curves at 4.2 K are observed only in the case of orientation of the field along axis $\langle 111 \rangle$ namely two jumps. Upon attainment of the compensation point T_c , the temperature at which the magnetizations of the RE and iron sublattices, in the absence of a field, are equal and opposite in direction, the number of jumps increase to three in the case $H \parallel \langle 111 \rangle$, while one and two jumps, respectively, appear for orientation of the field along axes $\langle 100 \rangle$ and $\langle 110 \rangle$. On further increase of temperature, the anomalies of the magnetization disappear on attainment of the critical temperature T_{cr} , along all three axes.

Similar diagrams are observed for all compositions with $x > x_c$. For compositions with $x > 1.25$, in fields attainable in our experiments, phase diagrams can be traced only near the compensation point T_c . The results obtained in the investigation of $\text{Ho}_3\text{Fe}_5\text{O}_{12}$ agree well with literature data.³

2. CALCULATION OF H - T - x PHASE DIAGRAMS

The present paper is a natural continuation of the previous paper¹; therefore we shall leave the notation for physical quantities as before: $M_{Fe} = 5\mu_B$ is the resultant magnetic moment of the iron sublattices, per formula unit; μ_R is the magnetic moment of a RE ion; H_{mol} is the molecular field exerted on the RE ions by the iron sublattice, which we take equal to 125 kOe.² As before,¹ we restrict ourselves to a model in which

the magnetic ordering of the RE ions is of Ising character; this should occur when the lower levels of the ion in the crystal field are two singlets close to each other (a quasideublet), sufficiently separated from the higher-placed levels.⁴ Nekvasil⁵ showed that the electronic levels of the Ho^{3+} ion in the garnet structure answer to this requirement. The Ising axes for each of the three sublattices of Ho^{3+} ions are axes z_i ($z_1 \parallel \langle 001 \rangle$, $z_2 \parallel \langle 100 \rangle$, $z_3 \parallel \langle 010 \rangle$). We represent the thermodynamic potential of the system per molecule, in the case of finite temperatures, in the form

$$\Phi = -M_{Fe}H - \frac{xT}{3} \sum_{i=1}^3 \ln 2 \text{ch} \frac{\mu_R(H + H_{mol})z_i}{T}.$$

In the dimensionless variables $f = \Phi/M_{Fe}H_{mol}$, $h = H/H_{mol}$, $\tau = T/\mu_R H_{mol}$, $a = x\mu_R/3M_{Fe}$, the thermodynamic potential for each of the three field orientations $\langle 001 \rangle$, $\langle 111 \rangle$, and $\langle 110 \rangle$ takes the form

$$f_{001} = -h \cos \theta - \tau a \left[2 \ln \text{ch} \frac{\sin \theta}{2^{1/2}\tau} + \ln \text{ch} \frac{h - \cos \theta}{\tau} \right];$$

$$f_{111} = -h \cos \theta - \tau a \left[\ln \text{ch} \frac{h - \cos \theta \pm 2^{1/2} \sin \theta}{3^{1/2}\tau} + 2 \ln \text{ch} \frac{h - \cos \theta \mp 2^{1/2} \sin \theta}{3^{1/2}\tau} \right];$$

$$f_{110} = -h \cos \theta - \tau a \left[\ln \text{ch} \frac{\sin \theta \sin \varphi}{\tau} + \ln \text{ch} \frac{h - \cos \theta - \sin \theta \cos \varphi}{2^{1/2}\tau} + \ln \text{ch} \frac{h - \cos \theta + \sin \theta \cos \varphi}{2^{1/2}\tau} \right].$$

In the case $H \parallel \langle 001 \rangle$, the coordinates of the vector M_{Fe} are determined, in a system of coordinates with axes $\langle 100 \rangle$, $\langle 010 \rangle$, $\langle 001 \rangle$, by the usual method of introducing polar and azimuthal angles θ and φ . For $H \parallel \langle 111 \rangle$, the corresponding axes are chosen along directions $\langle 1\bar{2}1 \rangle$, $\langle 01\bar{0} \rangle$, and $\langle 111 \rangle$; and for $H \parallel \langle 110 \rangle$, along $\langle 1\bar{1}0 \rangle$, $\langle 00\bar{1} \rangle$, and $\langle 110 \rangle$. In writing the expression for f_{001} we have taken into account that, as analysis has shown, the motion of the moment M_{Fe} occurs in one of the four equivalent half-planes of the type (110), i. e., $\varphi = (\pi/4)(2k+1)$, $k=0, 1, 2, 3$; this is a consequence of the fact that the axes of type $\langle 100 \rangle$ are symmetry axes of the fourth order. In the case $H \parallel \langle 111 \rangle$ the motion of the vector M_{Fe} again occurs in one of the planes of type (110); but, for example, the half-plane $\varphi=0$ is no longer equivalent to the half-plane $\varphi=\pi$; this accounts for the appearance of corresponding upper and lower signs in the expression for f_{111} . This affects the direction of initial motion of the vector M_{Fe} : clockwise or counterclockwise in the (110) plane, depending on the concentration, the temperature, and the value of the field. For $H \parallel \langle 110 \rangle$, the expression for f_{110} takes into account that the moment M_{Fe} may deviate from a plane of type (110) ($\cos \varphi=0$) by an angle $|\Delta\varphi| < \pi/2$, depending on h , τ , and x .

To plot H - T - x diagrams, the extremum problem for the thermodynamic potential was solved on a computer for those concentrations for which measurements were made. Along with the phase-transition lines, we calculated the boundaries of the regions of existence of the phases, characterized by the direction of the magnetic moments of the Ho^{3+} ions in each of the three sublattices.

tices. In each phase, the values of the angles θ and φ were determined in the $h\tau$ plane, and the equilibrium resultant magnetizations and susceptibilities were calculated. This information gives a complete picture of the phase transitions of the first and second kinds. Thus overlapping of the regions of existence of the phases in the vicinity of a line of phase transition indicates that this is a line of phase transition of the first kind, and along with the field dependence of the angle it enables us to determine the end of the line of phase transition of the first kind.

In the extrapolation of the lines of phase transition to absolute zero of temperature, the results of the earlier paper¹ were used.

3. ANALYSIS OF THE BEHAVIOR OF PHASE-TRANSITION LINES IN THE H - T - x DIAGRAMS

Since, in the model adopted, the Ho^{3+} ions are treated in the Ising approximation, the magnetic phase transformations in this system can occur only by discrete reorientations of the magnetic moments of the holmium ions in one or several sublattices to the opposite directions (with a corresponding change of \mathbf{M}_{F_e}). Such phase transitions at $T=0$ are accompanied by reorientation of the resultant magnetic moment \mathbf{M}_R of the Ho^{3+} ions from one direction of type $\langle 111 \rangle$ to another. When $T \neq 0$, flip of the magnetic moments of the Ho^{3+} ions in any sublattices because of a change of orientation of \mathbf{M}_{F_e} is accompanied by a change of the moduli of the magnetic moments of the Ho^{3+} ions in all the sublattices, so that, except for the collinear phases, \mathbf{M}_R will no longer be oriented along directions of type $\langle 111 \rangle$. We shall label the phases in accord with the projections of the magnetic moments of the Ho^{3+} ions on the Ising axes in each of the sublattices:

$$\nu_i = \text{sign } M_{Ri} z_i = \text{sign } (\mathbf{H} + \mathbf{H}_{\text{mol}}) z_i.$$

The phase diagrams for the three orientations of the external magnetic field indicated above are given in Figs. 1 and 2. For illustration, the concentrations $x = 0.67 < x_c$ and $x = 1.05 > x_c$ were chosen. We shall consider in sequence the diagrams for the three orientations of the external field.

A. $\mathbf{H} \parallel \langle 111 \rangle$. A typical diagram for the case $x < x_c$ is represented in Fig. 1a. For definiteness, we shall consider reorientation of the magnetic moment of the iron ions in the plane (110) . The line $A'Q$ in Fig. 1a separates the collinear phase I ($\nu_1 = \nu_2 = \nu_3 = -1$ ($\mathbf{M}_{F_e} \parallel \mathbf{H}$, $\mathbf{M}_R \parallel -\mathbf{H}$)) from the angular phase II ($\nu_1 = 1$, $\nu_2 = \nu_3 = -1$). On this line, deviation of the vector \mathbf{M}_{F_e} from the field direction causes flipping of the magnetic moments of the Ho^{3+} ions in the first sublattice. The deviation of the vector \mathbf{M}_{F_e} occurs jumpwise: the angle θ changes by a certain value $\Delta\theta$ that increases with the concentration of RE ions and decreases with rise of temperature. The magnetic moment of the ferrimagnet behaves in similar fashion on the line of the first-order phase transition. At the critical point Q, the values of the jumps $\Delta\theta$ and ΔM vanish.

With increase of the magnetic field, the next first-order phase transition line is the line $A''Q$. On it there

occurs a phase transition from the angular phase II to the angular phase III ($\nu_1 = -1$, $\nu_2 = \nu_3 = 1$). Here the directions of the magnetic moments of the Ho^{3+} ions in all three sublattices change to the opposite directions.

On the line AQ , the vector \mathbf{M}_{F_e} discontinuously assumes a direction parallel to the direction of the external field, and as a result there occurs a flipping of the moments of the RE ions in the first sublattice; the system changes to the collinear phase IV ($\nu_1 = \nu_2 = \nu_3 = 1$, $\mathbf{M}_{F_e} \parallel \mathbf{H}$, $\mathbf{M}_R \parallel \mathbf{H}$).

On increase of the concentration x to the value x_c , a more and more pronounced maximum develops on the line AQ , and the line itself moves up somewhat (the magnetic field for transition to the collinear phase is increases). The critical temperature (the point Q), in accordance with the equality $\tau_{cr} = a$, varies linearly with the concentration:

$$T_{cr} = (\mu_R^2 H_{\text{mol}} / 3M_{F_e}) x. \quad (1)$$

The expression (1) is valid both for $x > x_c$ and for $x < x_c$, and also for the case $\mathbf{H} \parallel \langle 110 \rangle$.

An example of a diagram for a concentration $x > x_c$ is shown in Fig. 2a, where $x = 1.05$. The topology of this diagram is the same as for the H - T diagrams of yttrium-iron garnet.⁶ Below the point T_c , as the field H increases, the collinear phase I is absolutely stable: $\nu_1 = \nu_2 = \nu_3 = 1$ ($\mathbf{M}_{F_e} \parallel -\mathbf{H}$, $\mathbf{M}_R \parallel \mathbf{H}$). On the first-order phase-transition line $A'B$, a flip of the moments of the RE ions in the first sublattice occurs, and phase I transforms to the angular phase II: $\nu_1 = -1$, $\nu_2 = \nu_3 = 1$. As a result, the moment \mathbf{M}_{F_e} turns from the direction $\langle 111 \rangle$ toward the axis $\langle 1\bar{1}1 \rangle$. With increase of the field, the vector \mathbf{M}_{F_e} pulls itself closer and closer to the field direction; as a result, there again occurs a flip of the moments of the RE ions in the first sublattice, and on the line AQ there occurs a first-order phase transition to the collinear phase III: $\nu_1 = \nu_2 = \nu_3 = 1$ ($\mathbf{M}_{F_e} \parallel \mathbf{H}$, $\mathbf{M}_R \parallel \mathbf{H}$). Above T_c (point B on the diagram), we have $\mathbf{M}_{F_e} > \mathbf{M}_R$; and the situation is analogous to the case $x < x_c$ except that here the temperature and concentrations are higher, the decrease of the value of M_R with rise of temperature is appreciable, and therefore the phase-transition lines go more steeply to the critical point Q.

With increase of the concentration of Ho^{3+} ions when $x > x_c$, the point T_c (point B) moves along the temperature axis according to the law

$$T_c = \frac{2}{3^{3/4}} \mu_R H_{\text{mol}} \left[\ln \frac{x\mu_R + 3^{3/4} M_{F_e}}{x\mu_R - 3^{3/4} M_{F_e}} \right]^{-1} \quad (2)$$

the difference $T_{cr} - T_c$ decreases with increase of x . Therefore the loop BCQD in diagram 2a, moving toward larger T , shrinks and rotates counterclockwise about the point B.

B. $\mathbf{H} \parallel \langle 001 \rangle$. We first consider concentrations $x < x_c$. In this case, at temperatures less than a certain critical temperature T_{cr} (see below, Sect. 4), two angular phases exist, phase I ($\nu_1 < 0$) and phase II ($\nu_1 > 0$); their ranges of existence overlap. The transition from phase I ($\nu_1 < 0$) to phase II ($\nu_1 > 0$) is of first order.

As an example, the numerically calculated phase diagram for concentration $x=0.67$ is shown in Fig. 1b. The line KQ is a first-order phase-transition line between the angular phases I and II. Below the curve KQ , phase I ($\nu_1 < 0$) is absolutely stable; above it, phase II ($\nu_1 > 0$) is absolutely stable. At higher temperatures, on the line MM' the angular phase transforms smoothly (a second-order transition) to the collinear phase $\theta = 0$. With increase of x , the line KQ goes down to the temperature axis. At $x = x_c$, the line KQ will be a segment of a straight line passing through the origin of coordinates.

When $x > x_c$, the first-order phase transition line (the line KQ) goes out from the point T_c on the temperature axis (see Fig. 2b). When $T < T_c$, the magnetic moment of the iron ions, with increase of the field, is continuously reoriented from the direction of M_{F_0} at $H = 0$, $\langle 111 \rangle$, to the axis $\langle 001 \rangle$. When $T > T_c$, the picture is similar to the case $x < x_c$. With increase of the concentration of the Ho^{3+} ions, $\tau_c \rightarrow a$ and $\tau_c < \tau_{cr} < a$; therefore the first-order phase-transition line (the line KQ) shifts, with increase of x , along the temperature axis to the right, gradually becoming straight and departing from the temperature axis more steeply.

C. $H \parallel \langle 110 \rangle$. The numerically calculated phase diagram in this case, for $x = 0.67$, is shown in Fig. 1c. The phase-transition lines $A'Q$ and AQ separate the regions of absolute stability of the angular phases I ($M_R^{(2)} z_2 = M_R^{(3)} z_3 < 0$) and III ($M_R^{(2)} z_2 = M_R^{(3)} z_3 > 0$), in which the vector M_{F_0} is in the plane $(1\bar{1}0)$ ($\cos \varphi = 0$), from the angular phase II, in which the vector magnetization of the iron sublattice departs from this plane, being inclined at an angle $\Delta\varphi$. The line MM' is a second-order phase transition line separating the collinear phase ($\theta = 0$) from the angular phase. This line coincides with the analogous line for the case $H \parallel \langle 001 \rangle$, for any x , and is tangent to the line AQA' at the point Q . On the phase-transition lines $A'Q$ and AQ there are tricritical points, C' and C , at which the first-order phase transition lines change to lines of second order, so that the lines CQ and $C'Q$ are second-order phase-transition lines, while AC and $A'C'$ are lines of first order. With increase of x , the point A' goes down, reaching zero when $x = x_c$. On further increase of x , the points A and A' draw closer together, merging at $x = 0.9$ (see Ref. 1). When $x > 0.9$, the phase diagram in the HT plane is a closed loop, which at the point $h = 1$, $\tau = a$ is tangent to the second-order phase-transition line MM' .

Figure 2c shows the numerically calculated phase diagram for $x = 1.05$. To the left of the temperature corresponding to point Q' on the diagram, the vector M_{F_0} , with increase of the field, continuously reorients from the direction $M_{F_0} \parallel \langle 111 \rangle$ to the axis $\langle 110 \rangle$ in the plane $(1\bar{1}0)$. In the temperature range located below the temperature corresponding to the point Q' but less than T_c , reorientation of the moments of the RE sublattices occurs on first-order phase-transition lines: the vector M_{F_0} departs discontinuously from the $(1\bar{1}0)$ plane on the line BQ' and returns to it on the line AQ' . When $T > T_c$, the situation is similar to the case $x < x_c$. With

increase of the concentration of RE ions, the loop $BQ'AQ$ shifts along the T axis to the right, meanwhile shrinking.

4. BEHAVIOR OF HYIG IN THE VICINITY OF THE CRITICAL POINTS

On the phase diagrams under investigation, there are three types of critical points:

1. The point Q for $H \parallel \langle 111 \rangle$ (Figs. 1a and 2a). At this point, three first-order phase-transition lines terminate.
2. The point Q for $H \parallel \langle 001 \rangle$ (Figs. 1b and 2b). This point is a point of termination of a first-order phase transition line and is analogous to the well known critical point of the vapor-liquid type.
3. The point Q for $H \parallel \langle 110 \rangle$ (Figs. 1c and 2c). At this point, the second-order phase-transition lines converge; they are continuations of lines of first-order phase-transition lines and are separated from the latter by the tricritical points C and C' . Through the point Q also passes a line of phase transition of second order, separating the collinear phase from the angular phases.

To analyze the system near the critical points, we shall use the Landau theory of phase transitions.⁷

A. $H \parallel \langle 111 \rangle$. As transition parameter, vanishing at the critical point Q , we here take the angle θ . In the expansion of the thermodynamic potential in this parameter, it is sufficient to retain fourth-order terms:

$$\begin{aligned} f_{111} &\sim \frac{1}{2} \alpha \theta^2 + \frac{1}{3} \gamma \theta^3 + \frac{1}{4} \beta \theta^4; \\ \alpha &\approx 1 - a/\tau + 2a(h-1)^2/3\tau^2, \\ \gamma &\approx \pm 2^h a(h-1)/6\tau^2, \\ \beta &\approx a/6\tau^2 + 2a(h-1)/3\tau^2. \end{aligned}$$

The upper sign in the coefficient γ corresponds to the case $\varphi = 0$, the lower to $\varphi = \pi$. The standard procedure leads to the equations for the boundaries of the regions of stability of the collinear phase, $h_c(\tau)$, and of the angular, $h_{II}(\tau)$:

$$\begin{aligned} h_c &= 1 \pm [3/2(1-\tau/a)]^{1/2}, \quad \tau \leq a; \\ h_{II} &= 1 \pm 2[3/2(1-\tau/a)]^{1/2}, \quad \tau \leq a. \end{aligned}$$

These curves pass through the point Q with coordinates $\tau = a$, $h = 1$. The overlapping of the regions of stability indicates that the line AQA' in Figs. 1a and 2a is a line of a phase transition of first order. Its equation is

$$h_{AQA'} = 1 \pm [3(1-\tau/a)]^{1/2}.$$

The jumps of the transition parameter during the transitions across the lines $A'Q$ and AQ are the same, in the neighborhood of Q , and are

$$\Delta\theta = 2^h |h_{AQA'}(\tau) - 1|/3.$$

The projections of the magnetic moment (per formula unit) on the field direction undergo, on transition cross these lines, jumps determined by the formula

$$\Delta M_{AQA'} = 3a(1-\tau/a)^2.$$

On the diagram 1a there is still another first-order phase transition line, viz., the line $A''Q$, passing in the vicinity of the point Q along the line $h = 1$, on which

the vector M_{F_0} changes from the region where $\varphi = 0$ and $h < 1$ to the region where $\varphi = \pi$ and $h > 1$; on the line $h = 1$, the angle θ is

$$\theta_{A \rightarrow Q} = 3(\tau^2/a^2) [(1-\tau/a)/6]^{-1/2},$$

and the discontinuity of the projection of the vector M_{F_0} on the direction $\langle 111 \rangle$ is

$$\Delta M_{A \rightarrow Q} = (3\tau^2/a) [3(1-\tau/a)]^{1/2} [1+a^2/108\tau^2].$$

B. $H \parallel \langle 001 \rangle$. We shall determine the position of the critical point $Q(\tau_{cr}, h_{cr})$ in this case. At the point Q , the angular jump $\Delta\theta$ vanishes. The magnetization jump ΔM also vanishes at this point. And since the first-order phase-transition line separates the regions with $M_R^{(1)} z_1 < 0$ and with $M_R^{(1)} z_1 > 0$, the critical point Q can be defined as the point of loss of stability of the solution $\theta = \theta(h, \tau)$ for which

$$M_R^{(1)} z_1 = a \operatorname{th} [(h - \cos \theta)/\tau] = 0,$$

i. e., $h = \cos \theta$. On minimizing the thermodynamic potential f_{001} and using the condition $h = \cos \theta$, we find that the position of the critical point is determined by the following equations:

$$\tau = [2(1-h^2)]^{1/2} \ln^{-1} \{ [2^{1/2} a + (1-h^2)^{1/2}] / [2^{1/2} a - (1-h^2)^{1/2}] \}; \quad (3)$$

$$h^2(1-h^2) - 2a(a-\tau) = 0, \quad (4)$$

where (3) is the line on which $M_R^{(1)} = 0$, while (4) is the condition for loss of stability of this solution.

The system (3)–(4) admits the solution $\tau = a$, $h = 1$. But as analysis has shown, this point (corresponding to the critical point for field directions $\langle 111 \rangle$ and $\langle 110 \rangle$) is not the critical point sought in our case, but represents the point at which the solution $M_R^{(1)}$ in the angular phase ($h = \cos \theta(h, \tau)$) changes smoothly, by a transition of second order, to the solution $M_R^{(1)} = 0$ in the collinear phase ($\theta = 0$, $h = 1$).

As was mentioned above, on the phase diagram there is still another line, the second-order phase transition MM' . On it the angle θ taken as transition parameter approaches zero continuously. An expansion of thermodynamic potential f_{001} is carried out in even powers of θ through the sixth degree. As a result of minimization, we arrive at the following equation for the line MM' in the vicinity of the point L ($\tau = a$, $h = 1$), through which it passes:

$$h_{MM'} = 1 - [6(a-\tau)]^{1/2} \tau. \quad (5)$$

C. $H \parallel \langle 110 \rangle$. For this field direction, it is convenient to introduce a two-dimensional transition parameter: $p = \theta \sin \varphi$, $q = \theta \cos \varphi$. In the vicinity of the critical point Q , the thermodynamic potential is represented in the form

$$f_{110} \sim 1/2 \alpha_p p^2 + 1/2 \alpha_q q^2 + 1/4 \beta_p p^4 + 1/4 \beta_q q^4 + 1/2 \delta p^2 q^2$$

with expansion coefficients

$$\alpha_p \approx (1-a/\tau) + a(h-1)^2/6\tau^2; \quad \alpha_q \approx a(h-1)^2/2\tau^2 + \alpha_p;$$

$$\delta \approx -a(h-1)^2/3\tau^2 + a(h-1)^2/12\tau^2 + a(h-1)/2\tau^2 - \alpha_p/6;$$

$$\beta_p \approx a(h-1)^2/4\tau^2 + a/3\tau^2 - \alpha_p/6;$$

$$\beta_q \approx -2a(h-1)^2/3\tau^2 - a[1+2/\tau^2](h-1)^2/12\tau^2 + a(h-1)/\tau + a/6\tau^2 - \alpha_p/6.$$

All the lines in the vicinity of the point Q are phase 0

transition lines of second order. The equation for the line MM' coincides exactly with equation (5). This line separates the collinear phase from the angular phase in which the vector M_{F_0} lies in a plane of the type (110); and only at the critical point does this phase touch the phase in which M_{F_0} is not in this plane. The equation of the line CQC' , which separates the two angular phases and which goes through Q , has (in the vicinity of Q) the form

$$h = 1 \pm [2(1-\tau/a)]^{1/2} \tau, \quad \tau \leq a.$$

To determine the tricritical points, we note that the parameter θ is not small in the vicinity of the points C and C' . Therefore it is necessary to consider a one-parameter expansion of the thermodynamic potential, in the parameter $\zeta = \cos \varphi$, which approaches zero continuously on the line CQC' of phase transition of second order:

$$f_{110} \sim 1/2 \alpha \zeta^2 + 1/4 \beta \zeta^4 + \dots$$

According to Landau's theory of phase transitions,⁷ at the tricritical points $\alpha = \beta = 0$; this leads to the system of equations

$$\operatorname{th} \xi / \xi = 1 - \operatorname{th}^2 \kappa, \quad (6)$$

$$-\operatorname{th} \xi / \xi^3 + (1 - \operatorname{th}^2 \xi) / \xi^2 = 1/2 (\operatorname{th}^2 \kappa - 1) (3 \operatorname{th}^2 \kappa - 1), \quad (7)$$

in which, for brevity, we have used the notation $\xi \equiv \sin \theta / \tau$, $\kappa \equiv (h - \cos \theta) / 2^{1/2} \tau$.

For solvability of the problem posed, we write still another equation, a necessary condition for stability of the system on the line CQC' : namely $(\partial f_{110} / \partial \theta)_{\zeta=0}$, or

$$\xi h \tau - a \operatorname{th} \xi [1 - \xi^2 \tau^2]^{1/2} - 2^{1/2} a \xi \tau \operatorname{th} \kappa = 0. \quad (8)$$

Eliminating κ from equations (6) and (7), we arrive at the transcendental equation for ξ

$$\frac{1}{\xi} - \frac{1}{\operatorname{th} \xi} + 2 \operatorname{th} \xi = \frac{2}{3}$$

with the solution $\xi \approx 0.482 \dots$. Further, we find from (6)

$$\kappa_i = 1/2 \ln [(1 + \epsilon_i) / (1 - \epsilon_i)], \quad i = 1, 2;$$

$$\epsilon_{1,2} = \pm [1 - \operatorname{th} \xi / \xi],$$

and then

$$h_i = 2^{1/2} \kappa_i \tau + [1 - \xi^2 \tau^2]^{1/2}, \quad (9)$$

here $h_1 > \cos \theta$ and $h_2 < \cos \theta$. Eliminating the field from equations (8) and (9), we arrive at a transcendental equation for the temperature at the tricritical point:

$$[1 - a \operatorname{th} \xi / \xi \tau] [1 - \xi^2 \tau^2]^{1/2} + 2^{1/2} \kappa_i \tau = 2^{1/2} a \epsilon_i.$$

Knowing the temperature, we find the field from (9); and from the definition of ξ we can find the angle θ .

In concluding this section, we note that on the second-order phase transition lines CQ and CQ' , as analysis on the stability of the system has shown, as a result of departure of the vector M_{F_0} from a plane of the type (110), the condition $M^{(2)} = M_R^{(3)}$ is violated: the magnetic moments of the second and third sublattices of RE ions change their values differently with change of field and temperature.

CONCLUSION

Our comparison of experimental data with theoretical results shows qualitative agreement; and at low concentrations, also quantitative. But there are a number of facts that cannot be explained in the model based on an Ising type of magnetic ordering of the Ho^{3+} ions in the garnet structure. This, for example, the experimental critical points are all of the same order of magnitude, whereas in the theory the critical point for $\text{H} \parallel (001)$ lies lower than for the other magnetic-field directions. The critical temperatures given by the Ising model in the case of field directions $\langle 111 \rangle$ and $\langle 110 \rangle$ are higher than the experimental. Thus although for concentration $x=0.67$ the numerical results for the proposed model are close to the experimental, for concentration $x=1.05$ the disagreement between theory and experiment for T_{cr} (in the case of these field directions) is ~ 7 K. This is especially noticeable for the loop in Fig. 2c.

The deviations from experiment can be explained as follows. We carried out the analysis of the phase diagrams by considering only the ground quasi-doublet of the Ho^{3+} ions in the crystalline field, neglecting the influence of the higher-placed levels. Allowance for higher-lying levels will lead to a faster decrease of the moment of the RE sublattices with increase of temperature, and consequently to a lowering of T_{cr} . Furthermore, as was mentioned earlier,¹ when $x > x_c$ the external field is parallel to the exchange field and causes one of the components of the quasidoublet to draw nearer to the higher-lying levels, and with increase of temperature the sharpest deviation from the theoretical model should therefore be observed precisely in the upper right part of the H - T diagram. Both of these factors leads to the result that compensation of the moments

of the RE and iron sublattices sets in at a lower T as compared with the model.

As calculations show, the presence of a gap of order 5 cm^{-1} (such a value for the energy of the gap follows from data of other authors⁵) has practically no effect on the quantitative calculations for $x \leq 0.1$. Therefore the model uses only the following parameters: H_{mol} , μ_R and M_{Fe} . Qualitative agreement with experiment is then observed up to concentration $x=1.25$. In fact, the behavior of the experimental lines of phase transitions on the H - T - x diagrams corresponds to the behavior of the calculated lines of phase transitions given by this simple model.

- ¹V. I. Silant'ev, A. I. Popov, R. Z. Levitin, and A. K. Zvezdin, Zh. Eksp. Teor. Fiz. 78, 640 (1980) [Sov. Phys. JETP 51, 323 (1980)].
- ²V. G. Demidov, Author's abstract of candidate's dissertation, Moscow State University, 1977.
- ³R. Z. Levitin and Yu. F. Popov, in: Ferrimagnetizm (Ferrimagnetism), Moscow State University, 1975, p. 6.
- ⁴J. S. Griffith, Phys. Rev. 132, 316 (1963).
- ⁵V. Nekvasil, Phys. Status Solidi (b) 94, K41 (1979); P. Novák, V. Nekvasil, T. Egami, P. J. Flanders, E. M. Gyorgy, and L. G. Van Uitert, Abstracts of Conference of CMEA (Council for Mutual Economic Assistance, Sovet ékonomicheskoi'vzaimopomoshchi, SEV) Countries on Physics of Magnetic Materials, Jaszowiec, Poland, 1980, p. I-17; P. Novák, V. Nekvasil, T. Egami, P. J. Flanders, E. M. Gyorgy, L. G. Van Uitert, and W. H. Grodkiewicz, J. Magnetism and Magnetic Materials 22, 35 (1980).
- ⁶R. Alben, Phys. Rev. B2, 2767 (1970).
- ⁷L. D. Landau and E. M. Lifshitz, Statisticheskaya fizika (Statistical Physics), 3d ed., M.: Nauka, 1976, Part 1, p. 486 (transl., Pergamon Press, 1980).

Translated by W. F. Brown Jr.

Investigation of the structure of some smectic A , B , and E phases

L. I. Mineev, L. A. Val'kova, L. S. Shabyshev, and I. G. Chistyakov

Ivanovo State University

(Submitted 8 September 1980)

Zh. Eksp. Teor. Fiz. 80, 1963-1968 (May 1981)

The structures of the smectic A , B , and E phases of butyl p -phenylbenzal- p' -aminocinnamate (BPBAC) oriented by a magnetic field are investigated by x-ray diffraction and microscopic analysis. It is observed that the ordering of the molecular structure of the E phase is higher than that of the high-temperature A and B phases. An attempt is made to describe the smectic E phase by means of a three-dimensional rhombic lattice structure. The optical analogy method is employed to verify the concepts regarding the structure of the smectic phases. On the basis of this investigation one can ascribe to the A , B , and E phases, symmetry symbols derived from the statistical distribution functions namely $C(B)$: 2, $a/2$; $C(A_2)$: 2, $a/2$, and $C(A_1)$: 2, $b/2$ respectively.

PACS numbers: 61.30.Eb, 61.30.Gd

The goal of our work was to study the smectic structure of the fourth homolog in the n -alkyl p -phenylbenzal- p' -aminocinnamate (BPBAC) series. C_6H_5 - C_6H_4 -

$\text{CH}-\text{N}-\text{C}_6\text{H}_4-\text{CH}-\text{CH}-\text{CO}\cdot\text{OC}_4\text{H}_9$, which has a smectic E phase in addition to A and B mesophases. The synthesis and identification of the mesophases of this ma-